Integrated compounding and injection moulding of short fibre reinforced composites

R. A. Sousa*[1,2], R. L. Reis[1], A. M. Cunha[1] and M. J. Bevis[2]

Composites of high density polyethylene (HDPE) and carbon fibre (C fibre) were compounded and moulded into tensile test bars in compounding injection moulding (CIM) equipment that combines a twin-screw extruder and an injection moulding unit. Two HDPE grades exhibiting different rheological behaviours were used as matrices. The mechanical properties of the moulded parts were assessed by both tensile and impact tests. The respective morphologies were characterised by scanning electron microscopy (SEM) and the semicrystalline structures of the matrices investigated by X-ray diffraction. The final fibre length distribution and fibre orientation profiles along the part thickness were also quantified. The composites with lower viscosity exhibit higher stiffness, higher strength and superior impact performance. Both composites exhibit a three layer laminated morphology, featuring two shell zones and a core region. Interfacial interaction is favoured by a lower melt viscosity that enhances the wetting of the fibre surfaces and promotes mechanical interlocking. The composites display a bimodal fibre length distribution that accounts for significant fibre length degradation upon processing. The dimensions of the transversely orientated core differ for the two composites, which is attributed to the dissimilar pseudoplastic behaviour of the two HDPE grades and the different thermal levels of the compounds during injection moulding. Further improvements in mechanical performance are expected through the optimisation of the processing conditions, tailoring of the rheological behaviour of the compound and the use of more adequate mould designs.

1 **Keywords:** PRC/2106

Introduction

Bone is a complex composite material composed of a polymeric matrix (collagen fibrils) and an inorganic stiff phase (hydroxyapatite crystals – HA)[1–3] that exhibits high stiffness and strength, strong anisotropy and a pronounced viscoelastic character. Based on these premises, Bonfield proposed the composites of high density polyethylene (HDPE) with hydroxyapatite (the main constituent of human bone) as hard tissue replacement materials.[4] The so-called bone–analogue composite combines a ductile polymeric phase with a stiff ceramic that establishes a direct analogy with the main bone constituents. The long term replacement of bone parts/defects requires mechanically biocompatible materials, i.e. materials that exhibit a bone-matching mechanical performance. In spite of the chemical affinity of these composites to human bone, the respective mechanical performance is far below the envisaged range of stiffness, 7–25 GPa.[5,6] Within this context, the possibility of using HDPE/HA composite systems in high load bearing applications depends on the technological ability of being able to produce components with complex geometry, specific tailored chemical properties and adequate mechanical behaviour. Attempts to extend the mechanical performance of HDPE/HA composites, in order to meet the envisaged mechanical requirements, have been based on the use of hydrostatic extrusion[7,8] and shear controlled orientation in injection moulding (SCORIM).[9,10] In both cases, the main objective was to develop a high level of orientation in the HDPE matrix through control of the respective structure development during processing, in order to mimic the bone anisotropy. For the case of SCORIM, the enhancement in mechanical performance (as compared to conventional moulding routes) is associated with the shear induced crystallisation of the HDPE phase as a result of the specific moulding environment.[10,11] In spite of these promising results, the stiffness exhibited by these composites is still compromised by the low aspect ratio of the particulate HA and the low level of interfacial interaction between these and the polymer matrix. In order to overcome such limitations, additional enhancements in the mechanical performance of HDPE/HA

[1]Department of Polymer Engineering, University of Minho, 4800-058 Guimarães, Portugal
[2]Wolfson Centre for Materials Processing, Brunel University, Uxbridge, Middlesex, UB8 3PH, UK

*Corresponding author. Current address: 3B's Research Group – Biomaterials, Biodegradables and Biomimetics, Department of Polymer Engineering, Campus de Gualtar – University of Minho, 4710-057 Braga, Portugal, email rasousa@dep.uminho.pt

Published by Maney on behalf of the Institute
Received 19 August 2004; accepted 15 September 2004
DOI 10.1179/174328904X3630

Plastics, Rubbers and Composites prc2106.3d 7/10/04 17:27:41
The Charlesworth Group, Wakefield +44(0)1924 369598 - Rev 7.51n/W (Jan 20 2003)

composites have relied on the control of both the interfacial interaction and the filler dispersion by the use of coupling agents.[10] Further improvements in mechanical performance are expected through the use of more efficient reinforcement strategies. A complementary approach to the previous one is the selective reinforcement of the core of the composites, where the use of HA is redundant, with very stiff reinforcements such as carbon fibres (C fibres). The combination of these two approaches should enable the development of bi-composite mouldings with controlled orientation, featuring: (i) an outer layer based on a HDPE/HA composite that assures the bioactive character of the implant; and (ii) a very stiff HDPE/C fibre composite core that determines most of the mechanical performance.[12]

This work reports an investigation on the processing and characterisation of such HDPE/C fibre composites. It was proposed to use these materials in the core of the previously mentioned bi-composite mouldings. Two HDPE grades exhibiting different rheological behaviours were chosen as polymer matrices. In order to retain the fibre integrity as much as possible and maximise the mechanical performance of these composites, a compounding injection moulding (CIM) apparatus, combining a twin-screw extruder and an injection moulding unit, was used. The mechanical properties of the moulded specimens were assessed by both tensile and impact tests. The morphology of the mouldings was characterised by scanning electron microscopy and the semicrystalline structure of the matrix investigated by X-ray diffraction. The final fibre length distribution and fibre orientation profiles along the part thickness were also quantified. The mechanical performance of both composites is discussed in terms of the morphology developed, structure of the semicrystalline matrix and final fibre characteristics.

Experimental

Materials

The HDPE grades studied were: (i) Hostalen GM 9255 F, supplied by Elenac GmbH (Germany) with a melt flowrate (MFR) of 0·37 ml/600 s (190°C, 5 kg) and (ii) Vestolen A 6016, supplied by Vestolen GmbH (Germany) with a MFR of 26 ml/600 s (190°C, 5 kg). The molecular weight characteristics of both HDPE grades are summarised in Table 1.

HDPE based composites were produced using chopped carbon fibres (C fibres) type HTA 5U41, supplied by Tenax Fibers, GmbH & Co. (Germany), with a length/diameter ratio (r_e) of 860. The physical characteristics of the C fibres are presented in Table 2.

Table 1 Molecular weight characteristics in terms of number averaged molecular weight (M_n), weight averaged molecular weight (M_w), polydispersity (M_w/M_n) and densities of HDPE grades studied

Grade	M_n	M_w	M_w/M_n	Density, g cm^{-3}
GM 9255 F	18 000	282 000	15·67	0·955
A 6016	56 212	58 000	1·03	0·962

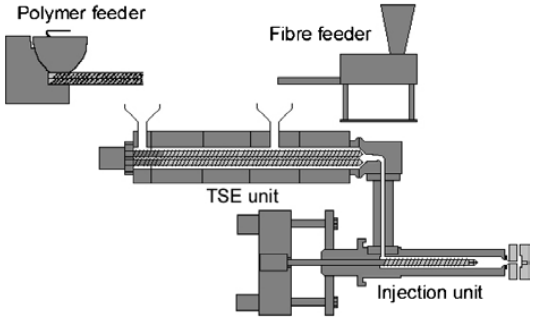

1 Schematic diagram of compounding injection moulding CIM equipment with in-melt feeding configuration and polymer and fibre feeder devices

Compounding injection moulding (CIM)

Compounding and injection moulding were performed in a single processing cycle, using an Osciblend compounding injection moulding machine (CIM) assembled by Dassett Processing Engineering Ltd (UK). It combines a modular corotating twin-screw extruder (TSE) with a screw diameter (D) of 40 mm and a length/diameter ratio (L/D) of 25 : 1, together with an injection moulding unit with 125 kN clamp force. The potential advantages of CIM for the processing of thermoplastics reinforced with short fibres, compared to separate compounding and injection moulding devices, are: single thermal history, superior maintenance of fibre morphology and elimination of fibre damage associated with extra granulation steps. A schematic diagram of the CIM equipment is presented in Fig. 1. During processing, the polymer pellets were fed by a T-35 volumetric feeder (K-Tron International). A continuous weight proportioner, KDA-GL 30N (Engelhardt GmbH) was used for the in-melt feeding of the C fibres. The screw configuration used during compounding is schematically described in Fig. 2 and features: (i) a feeding zone for the initial conveying of the solid material; (ii) a melting section where the melting of the polymer pellets takes place; (iii) a venting zone where melt decompression occurs and the C fibres are fed; and (iv) a final pumping zone. The connection between the TSE and the injection moulding units is a cross-manifold fitted with a conveying screw operating at 50 rev min^{-1}.

Composites of HDPE with 20 wt-% C fibres were compounded and subsequently injection moulded into tensile test bars with a rectangular cross-section of 4×9 mm^2. The mould runner system featured runners and edge gates with identical trapezoidal cross-section of $4 \times 4(5)$ mm^2. The mould geometry employed is schematically presented in Fig. 3 together with cross-section dimensions of the tensile test bar and runner/gate.

The processing conditions used for compounding and injection moulding are presented in Table 3. They differ for the two HDPE grades, in terms of the

Table 2 Physical properties of TENAX HTA C fibres[13]

Tensile modulus, GPa	238
Tensile strength, MPa	3950
Elongation at break, %	1·5
Cut length, mm	6
Filament diameter, μm	7
Density, g cm^{-3}	1·77

Plastics, Rubbers and Composites prc2106.3d 7/10/04 17:28:00
The Charlesworth Group, Wakefield +44(0)1924 369598 - Rev 7.51n/W (Jan 20 2003)

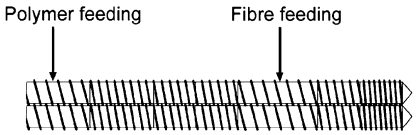

2 Schematic diagram of screw configuration employed for compounding

injection/holding pressure levels and the temperature profiles. The HDPE grade GM 9255 F requires higher processing temperatures and pressures as a result of its higher viscosity.

Tensile testing

The tensile tests were performed with an Instron 4505 tensile testing machine fitted with an Instron 2630 clip-on resistive extensometer with 10 mm of gauge length. In order to determine accurately the modulus, the elongation was measured by the extensometer at a crosshead speed of 5 mm min^{-1} ($8{\cdot}3 \times 10^{-5}$ m s^{-1}) until 1·5% strain. Beyond this strain value, the crosshead speed was increased to 50 mm min^{-1} ($8{\cdot}3 \times 10^{-4}$ m s^{-1}) and the extensometer was removed, the elongation being measured by the crosshead distance. The tangent modulus (E_t), the secant modulus at 0·8% strain ($E_{0{\cdot}8\%}$), the ultimate tensile strength (UTS), the strain at peak (ε_p) and the strain at break point (ε_b) were determined.

Impact testing

Impact tests were conducted in a Rosand Type 5 instrumented falling weight impact machine. The tests were performed at a test speed of 3 m s^{-1}, according to a three-point bending scheme, using a support with 32 mm span and a 25 kg anvil. For each test, the force at peak (F_p), the peak energy (U_p) and the failure energy (U_f) were determined. The force-deflection curves were acquired through a PC and displayed using a 8 kHz digital filter.

Scanning electron microscopy

Scanning electron microscopy (SEM) was performed for fractographic analysis on selected specimens with a Leica Cambridge LS360 scanning electron microscope. All the surfaces were mounted on a copper stub and coated by ion sputtering with an Au/Pd alloy before examination.

Sample preparation

The samples to be used in the X-ray diffraction experiments were obtained by cutting sections from the middle region of the gauge length of the tensile test bars. The sections were carefully polished until obtaining 1 mm thick specimens.

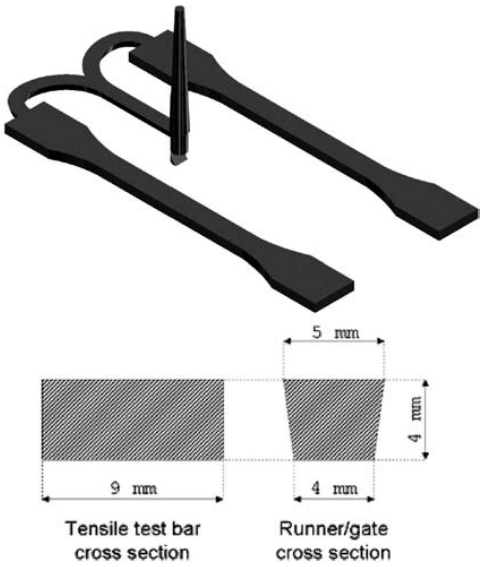

3 Schematic diagram of mould geometry employed together with cross-section dimensions of respective tensile test bars and runner/gate

The specimens for fibre orientation measurements were also obtained from the middle point of the gauge length of the bars. The sectioning of the specimens was performed at an angle α of about 45° (on average) relative to the machine direction, i.e. to the flow direction (and to the preferred fibre orientation). The sectioning of the specimens at an angle α is meant to increase the ellipticity of the fibres observed and minimise the orientation errors that arise because of the pixel nature of the acquired data images, as demonstrated elsewhere.[14] Figure 4 presents the definition of the transverse direction (TD), the normal direction (ND) and the machine direction (MD), and the respective relationship with the X, Y and Z axes used to define the fibre orientation, together with the definition of the sample cross-sectioning angle α. The sections obtained were immersed in an epoxy resin and, after curing of the resin, polished to produce a suitable surface for subsequent observation by optical reflectance microscopy.

Stereo light microscopy

The samples prepared according to the section 'Sample preparation' immediately above for use in the X-ray

Table 3 Processing composites of HDPE/C fibre composite

	Hostalen GM 9255 F	Vestolen A 6016
Compounding screw speed (rev min^{-1})	50	50
Injection pressure, MPa	20·0	16·0
Injection time, s	0·7	0·7
Holding pressure, stages 1 to 5, MPa	8·0/8·0/7·0/6·0/5·0	7·0/7·0/7·0/6·0/5·0
Holding pressure time, s	20	20
Cooling time, s	20·0	20·0
Temperature profiles*, °C	210/220/225/230, 235/235/240/245/250	145/180/195/205, 210/210/215/220/215
In-melt feeding temperature, °C	225	195

*From feed to die (underlined numbers correspond to the compounding unit).

Plastics, Rubbers and Composites prc2106.3d 7/10/04 17:28:01
The Charlesworth Group, Wakefield +44(0)1924 369598 - Rev 7.51n/W (Jan 20 2003)

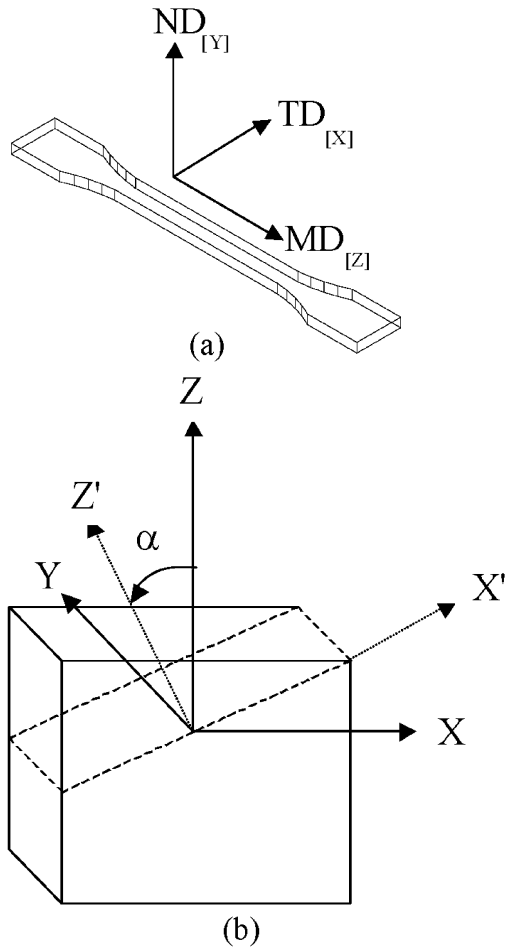

4 *a* Definition of machine direction (equivalent to main direction of flow – MD), transverse direction (TD) and normal direction (ND) relative to tensile bar and respective relationship with axes used to define fibre orientation; *b* sectioning of sample cross-section according to angle α defined between machine direction (MD – same as Z) and normal of section plane (Z′)

experiments were additionally observed by stereo light microscopy in a Nikon SMZ 10 microscope.

X-ray diffraction patterns

Ni filtered Cu K_α radiation with a wavelength of 0·1517 nm at 36 kV and 26 mA was used to obtain X-ray diffraction patterns in a Philips 1050 diffractometer. The patterns were acquired in order to assess the preferred orientation of the polymer matrix. The X-ray beam was oriented parallel to the thickness of the specimen and perpendicular to the flow direction. An aperture of 100 μm diameter was used to define the position and cross-section of the incident X-ray beam. The X-ray diffraction patterns were obtained for the mouldings at positions 0·1, 0·5, 1·0 and 4·0 mm from the edge of the mouldings.

Measurement of fibre orientation

The samples prepared according to the section 'Sample preparation' above were observed in an Olympus BH-1 microscope (reflectance mode) equipped with an image acquisition system composed of a Sony CCD camera and a PC fitted with a compatible video card. The images were acquired using objective and eyepiece magnifications of 20× and 10×, respectively. The pictures analysed had dimensions of 462 pixels × 712 pixels, which corresponds to a calibrated field of view of 165 μm × 254 μm. For each sample, the fibre orientation measurements were conducted in 13 layers along half of the thickness in three consecutive columns at the centre of the cross-section. The C fibres have a circular cross-section thickness that allowed for calculation of the respective orientation.

The calculation of the fibre orientation was based on the minor and major axes of the cross-section of the fibres observed as ellipses in the sectioned surface. The out-of-plane angle of a fibre θ' is given by

$$\theta' = \cos^{-1}\left(\frac{b}{a}\right) \tag{1}$$

where a and b are, respectively, the major and minor axes of the ellipsoid cross-section. For each layer, the measurements were performed for a single sectioning plane, which creates ambiguity in the out-of-diagonal tensor components, but which does not affect the diagonal tensor components. In this work, the out-of-plane angle θ' was assumed to be positive for all cases. The in-plane angle ϕ' was given by the angle between the major axis a of the ellipse and the X′ axis of the observation plane. The measurements of a, b and ϕ' were performed manually for each picture. As previously described in the section 'Sample preparation', the sectioning of the specimens at a certain angle α increased the ellipticity of the fibres observed and minimised the orientation errors that arise as a result of the pixel nature of the acquired images. However, the θ' and ϕ' angles describe the fibre orientation relative to a different coordinate system from the machine, transverse and normal directions. The transformation of the θ' and the ϕ' angles into the θ and ϕ values relative to the cross-section at right angles to the flow direction, i.e. along the X–Y plane, was performed according to the following expressions

$$\theta = \cos^{-1}\left(\sin\alpha.\sin\theta'.\sin\phi' + \cos\alpha.\cos\theta'\right) \tag{2}$$

$$\phi = \tan^{-1}\left(\frac{\cos\alpha.\sin\theta'.\sin\phi' - \sin\alpha.\cos\theta'}{\sin\theta'.\cos\phi'}\right) \tag{3}$$

During sample preparation, some variation around the value of α can occur. The determination of the α value for each sample was given by

$$\alpha = \cos^{-1}\left(\frac{x}{x'}\right) \tag{4}$$

where x is the actual width of the moulding cross-section and x' is the width of the observed cross-section after sectioning and polishing.

The fibre orientation in the mouldings was described by a second-order tensor, first proposed as descriptors of the state of orientation in composite materials by Advani and Tucker.[15] For the second-order tensor, each tensor component is defined by

$$a_{ij} = \langle p_i p_j \rangle \tag{5}$$

where p_i, p_j can be any of the p_1, p_2 or p_3 components of the vector $\boldsymbol{p}$ that describes the orientation of the fibre in the composite. The p_1, p_2 and p_3 components of the

Plastics, Rubbers and Composites prc2106.3d 7/10/04 17:28:04
The Charlesworth Group, Wakefield +44(0)1924 369598 - Rev 7.51n/W (Jan 20 2003)

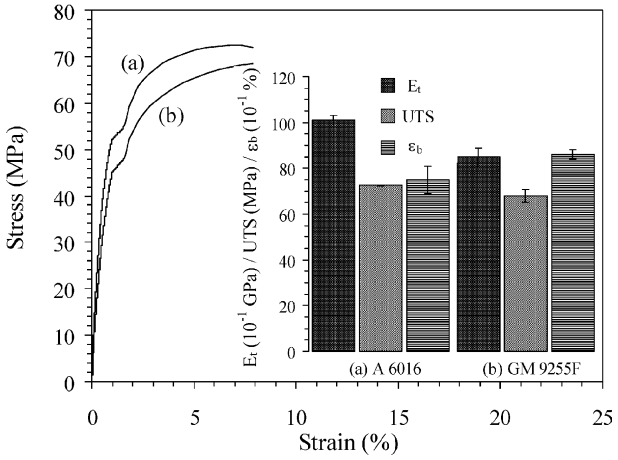

5 Typical tensile test curves of HDPE/C fibre composites for *a* A 6016 and *b* GM 9255 F matrices together with respective averaged values of E_t, UTS and ε_b

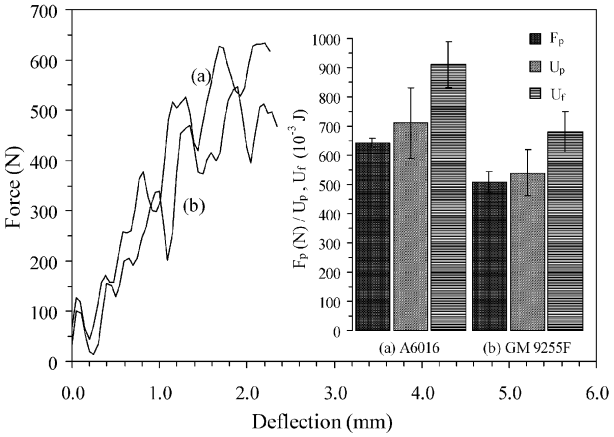

6 Typical impact test curves of HDPE/C fibre composites for *a* A 6016 and *b* GM 9255 F matrices together with respective averaged values of F_p, U_p and U_f

vector $\boldsymbol{p}$ are given by

$$p_1 = \sin\theta\cos\phi \tag{6a}$$

$$p_2 = \sin\theta\sin\phi \tag{6b}$$

$$p_3 = \cos\phi \tag{6c}$$

Determination of fibre length and fibre content

The determination of the fibre length in the moulded samples was performed after pyrolysis of the polymeric matrix for sections removed from the gauge length of the tensile test bars. For each specimen, the pyrolysis of the polymer matrix was conducted in an oven at 450°C for 4 h. The remaining fibres were immersed in acetone. The mixture obtained was then spread into a cover-glass and fibre length measurements were conducted after the evaporation of the solvent. The addition of acetone facilitated the spreading of the fibres and prevented any additional breakage. The fibres were observed in an Olympus BH-1 microscope (transmittance mode) equipped with an image acquisition system composed of a Sony CCD camera and a PC fitted with a compatible video card. For each specimen, a minimum of 600 fibres were measured and statistically analysed using SPSS v11·0 software. The weight fraction of the polymer matrix in the composites was determined by measuring, for each specimen, the weight loss upon pyrolysis. The C fibre fraction is readily calculated by subtracting this value from 1.

Results and discussion

Mechanical behaviour

Figure 5 presents the typical tensile curves for both the HDPE GM 9255 F/C fibres and the HDPE A 6016/C fibre composites, together with the respective average values of the tangent modulus (E_t), the ultimate tensile strength (UTS) and the strain at breaking point (ε_b). The GM 9255 F (higher molecular weight grade) based composites have a target modulus of 8·5 GPa and a UTS of 67·8 MPa. The composites with the A 6016 matrix (lower molecular weight grade) exhibit higher values of stiffness and strength with 10·1 GPa and 72·5 MPa for E_t and UTS, respectively. In terms of ductility, the HDPE GM 9255 F/C fibre composites exhibit a breaking strain of 8·6%, compared to 7·5% for the A 6016 based composites.

Density measurements conducted using the Archimedes principle gave the weight content of fibres for the A 6016 and the GM 9255 F based composites of 20·1% and 17·4%, respectively (n=5). The results from pyrolysis, obtained for a larger number of samples (n=10), differed from the density measurements. The fibre weight contents recorded for the A 6016 and the GM 9255 F based composites by this method were 18·7 and 19·3%, respectively. The difference observed between the two methods can be attributed to the existence of air voids and/or to eventual variations in the fibre content, which originated during the fibre feeding. The introduction of air may occur during polymer feeding before compounding of the polymer.[16] In spite of this fact, taking into account the pyrolysis experiments (for which a larger sample size has been used) the observed differences in tensile test behaviour between the two composites can hardly be explained by dissimilar C fibre contents.

The typical impact test curves for both the HDPE GM 9255 F/C fibres and the HDPE A 6016/C fibre composites are presented in Fig. 6, together with the respective average values of the force at peak (F_p), the peak energy (U_p) and the failure energy (U_f). The A 6016 based composites exhibit values of F_P and U_p of, respectively, 642 N and 0·71 J. The impact resistance of the GM 9255 F composites is considerably lower. For this composite, F_P and U_p are 508 N and 0·54 J, respectively. The superior impact performance of the A 6016 based composites is evidenced by the higher energy absorbed during crack propagation, U_f of 0·91 J, compared with 0·68 J for the GM 9255 F composites. It is evident from these results that the lower viscosity HDPE based composites exhibit a higher toughness.

The impact performance of semicrystalline polymers (assuming constant loading conditions) depends on a wide range of factors that include the morphology of the material, the structural characteristics of the crystalline/amorphous domains, the molecular weight of the polymer and the thermo-mechanical environment during

Plastics, Rubbers and Composites prc2106.3d 7/10/04 17:28:06
The Charlesworth Group, Wakefield +44(0)1924 369598 - Rev 7.51n/W (Jan 20 2003)

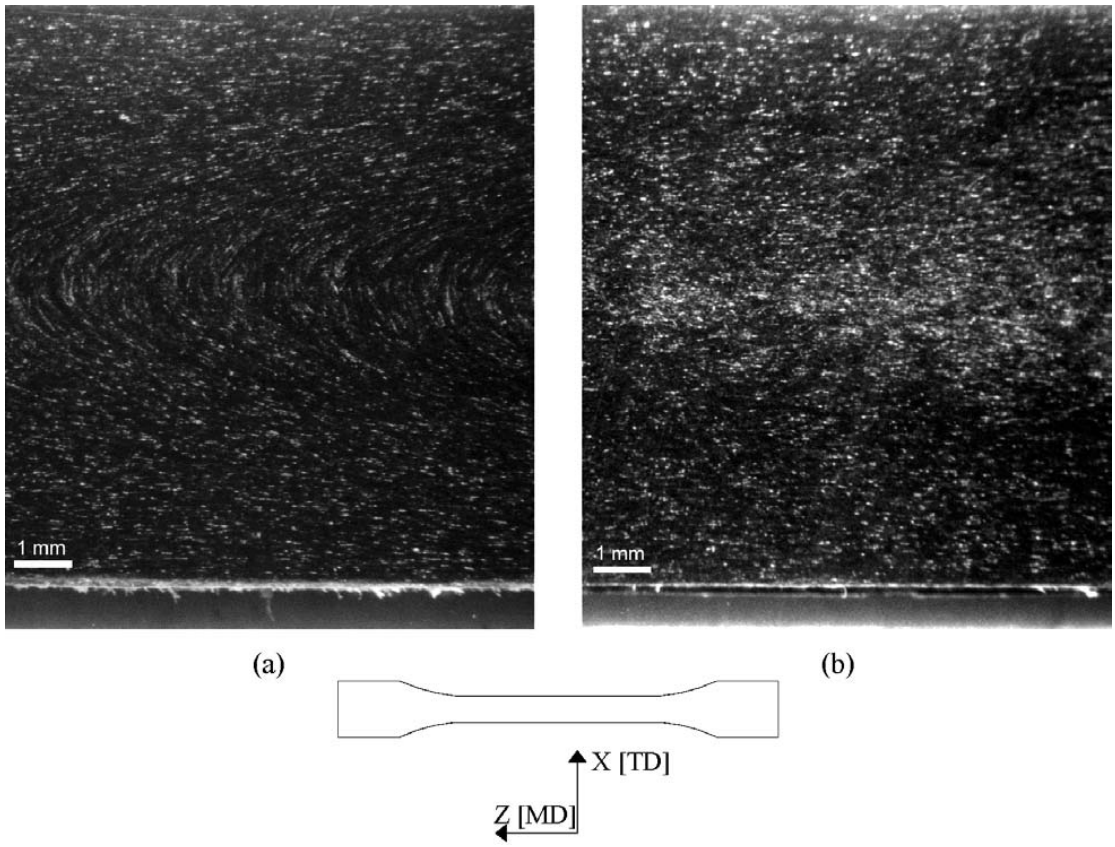

7 Longitudinal (X–Z plane) view of HDPE/C fibre composite mouldings: *a* GM 9255 F and *b* A 6016 matrices

processing.[17] This situation has further complexity in the case of composite materials, where factors such as the fibre length, the fibre orientation and the matrix/fibres interfacial interaction have to be taken into account.

Assuming identical final fibre characteristics (length and orientation) and fibre/matrix interaction for the two moulded composites, it could be possible, in theory, to infer the contribution of the HDPE matrix to the fracture process. A study by Egan and Delatycki[18] found the toughness of HDPE to depend on the dimensions of both the crystalline and amorphous domains and the weight averaged molecular weight (M_w). The molecular weight of the polymer appears to be a critical factor determining crack propagation.[19] A high molecular weight increases the density of tie molecules in the amorphous regions, which promote stress transfer upon loading of the material. Nevertheless, the role of molecular weight on the fracture propagation process cannot be considered in isolation, since it influences simultaneously the semicrystalline structure development during processing that also determines the fracture behaviour. Nevertheless, the lower impact performance of the HDPE GM 9255 F based composites is, initially, surprising when considering its higher molecular weight. The toughness of semicrystalline polymers is partially defined by two interrelated factors with opposite effects: crystallinity and lamellae thickness.[17] Considerable energy consumption occurs during deformation of the crystalline phase, which is reflected in a proportional relationship between crystallinity and toughness. However, increased crystallinity is associated with a higher lamellae thickness and a lower tie molecule density, which adversely affects the fracture behaviour beyond a critical value of crystallinity. The sum of these two competitive effects governs, in conjunction with the other previously mentioned factors, the toughness of the polymer. The fracture behaviour observed for the two polymers confirms that factors such as the crystallinity and lamellae thickness may have a crucial role on the determination of their impact behaviour.

Morphology developed and semi-crystalline structure exhibited

Figure 7 presents the stereo light microscopy photographs of the composite mouldings after longitudinal sectioning and polishing (X–Z plane). The HDPE GM 9255 F based composites (Fig. 7*a*) exhibit a symmetric laminated morphology featuring clear parabolic flow marks. This composite presents two distinct zones: a shell layer, where fibres appear to be predominantly parallel to the main direction of flow (MDF), and a core region, where the fibres are mainly transverse to the MDF. This laminated morphology is not evident for the A 6016 based composites (Fig. 7*b*).

Figures 8 and 9 combine the X-ray diffraction patterns with the respective scanning electron microscopy photographs of the tensile fracture surface for the GM 9255 F and A 6016 based composites, respectively. The laminated morphology of the HDPE GM 9255 F/C fibre composites is disclosed upon failure after tensile testing as can be observed in Fig. 8. In the vicinity of the mould wall, the fibres are predominantly orientated parallel to the MDF. In this region, the fibres exhibit evident signs of pull-out and debonding, which is an indication of low adhesion between the C fibres and the GM 9255 F matrix. At the moulding core, the fibres are predominantly orientated in the transverse

Plastics, Rubbers and Composites prc2106.3d 7/10/04 17:28:07
The Charlesworth Group, Wakefield +44(0)1924 369598 - Rev 7.51n/W (Jan 20 2003)

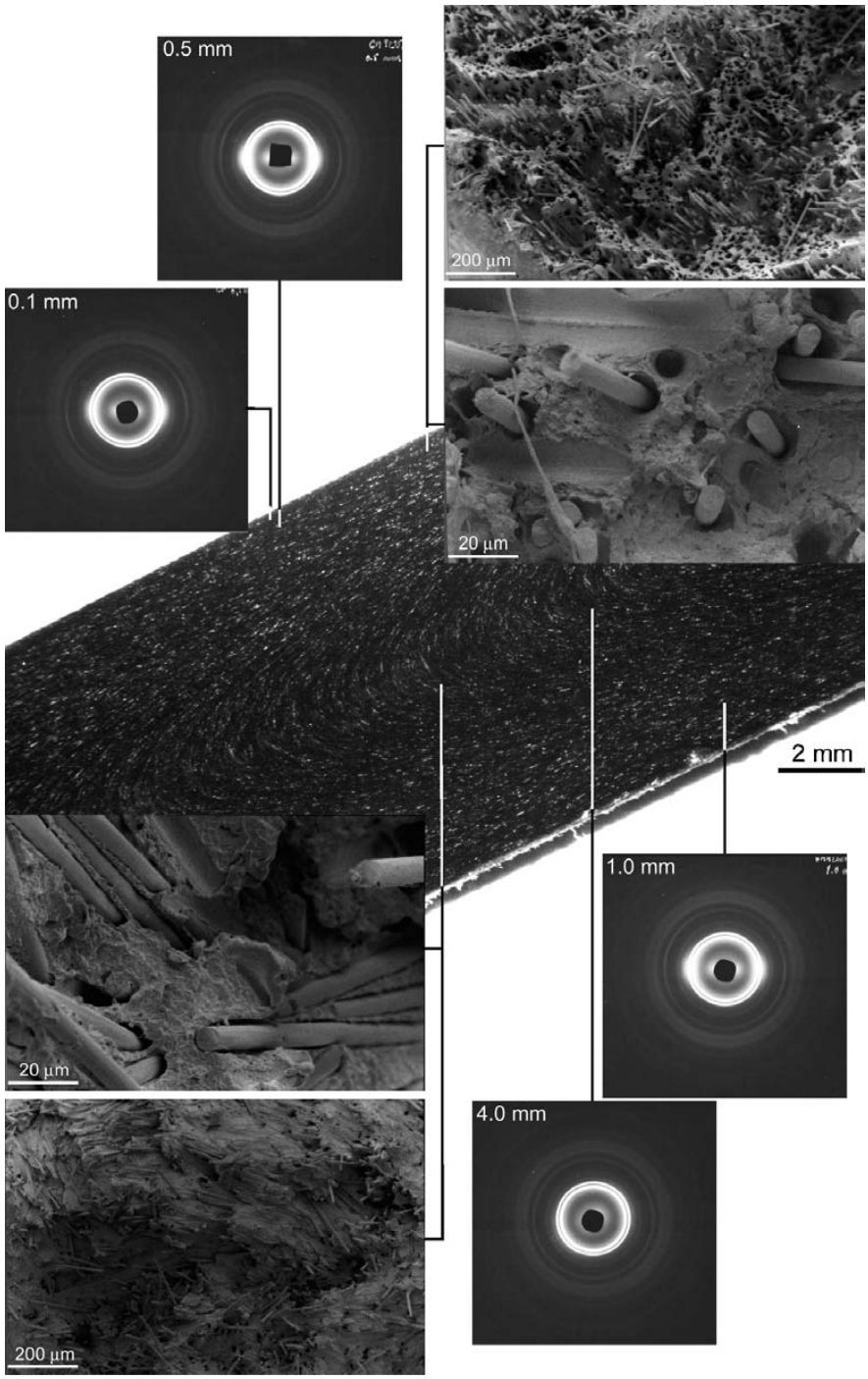

8 Longitudinal section of moulding, X-ray diffraction patterns at 0·1, 0·5, 1·0 and 4·0 mm from mould wall and typical tensile fracture surface at both skin and core regions for HDPE GM 9255 F/C fibre composite

direction to the MDF, i.e. to the loading direction during tensile testing. The laminated morphology observed here is typical of injection moulded short fibre reinforced composites[20–28] and can be described by a variant number of layers, depending on the description level adopted during characterisation.[25,29] This morphology is usually described as being comprised of five regions, namely two skin layers, two shell layers and a core region.[25] The skin is formed due to the elongational flow of the melt flow front that gives rise, upon rapid cooling of the material at the cavity surface, to a random-in-plane state of orientation of the fibres.[29,30] The existence of these skin layers is not evident in Fig. 8. Concerning the semicrystalline nature of the HDPE matrix, the X-ray diffraction patterns gained along the cross-section width reveal reduced molecular orientation. The higher intensity at the equator region for the (110) and (200) reflections suggests that C-axis orientation occurs for distances up to 1·0 mm from the mould wall. At the centre region of the moulding, no apparent crystalline anisotropy is present.

The HDPE A 6016/C fibre composites (Fig. 9) exhibit an identical laminate morphology to the GM 9255 F based composites comprising three regions: two shell zones and a core. The existence of a skin region is once again not confirmed by the SEM images. The fracture surfaces show an enhanced level of adhesion between the

Plastics, Rubbers and Composites prc2106.3d 7/10/04 17:28:09
The Charlesworth Group, Wakefield +44(0)1924 369598 - Rev 7.51n/W (Jan 20 2003)

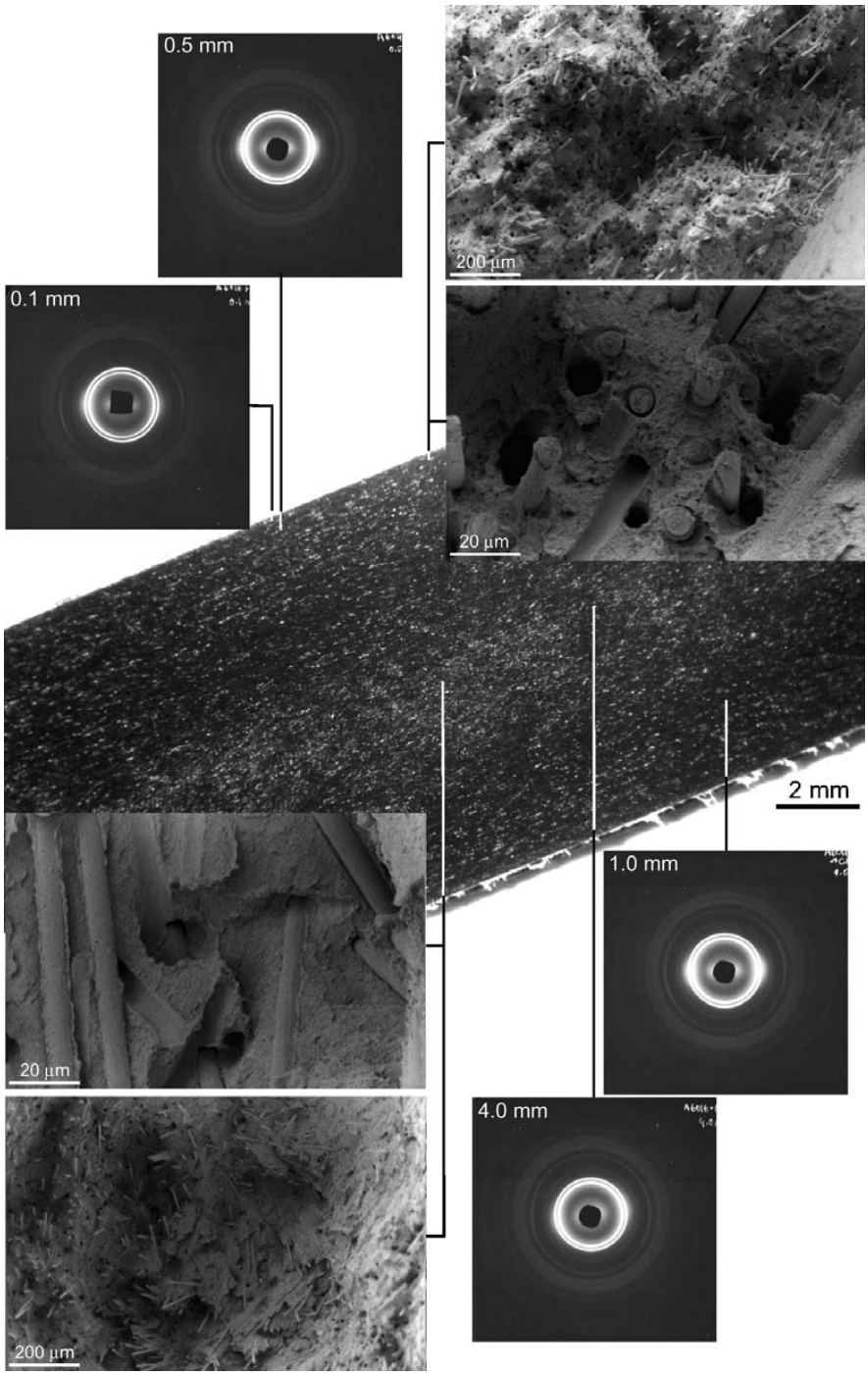

9 Longitudinal section of moulding, X-ray diffraction patterns at 0·1, 0·5, 1·0 and 4·0 mm from mould wall and typical tensile fracture surface at both skin and core regions for HDPE A 6016/C fibre composite

C fibres and the HDPE matrix at both the shell and the core regions compared to GM 9255 F based composites. As pointed out by Karger-Kocsis for polypropylene based composites,[31] the testing conditions determine the deformation mechanisms upon fracture, which in turn define the apparent level of adhesion between the phases observed during fractographic analysis. For the tensile testing conditions employed, the plastic deformation of the matrix upon loading is very significant, being accompanied by an extensive fibre pull-out. For these failure conditions, it is possible to evaluate on a comparative basis the fibre/matrix adhesion in the two composites. The apparent higher adhesion of the C fibres to the A 6016 HDPE grade is confirmed by observation of Fig. 10 that presents the C fibres/matrix interfaces for the GM 9255 F (Fig. 10*a*) and the A 6016 (Fig. 10*b*) based composite materials. The higher adhesion between the fibres and the A 6016 matrix is believed to result from the lower viscosity of this grade and the improved wetting that enhances mechanical interlocking between the two phases and favours stress transfer during loading. Similar to what is observed for GM 9255 F composites, the semi-crystalline structure of the A 6016 composites, assessed by X-ray diffraction (Fig. 9), exhibits signs of *c*-axis orientation close to the mould wall. The crystalline anisotropy results from the effect of shear at relatively small distances from the mould wall during the crystallisation process that results in the

Plastics, Rubbers and Composites prc2106.3d 7/10/04 17:28:13
The Charlesworth Group, Wakefield +44(0)1924 369598 - Rev 7.51n/W (Jan 20 2003)

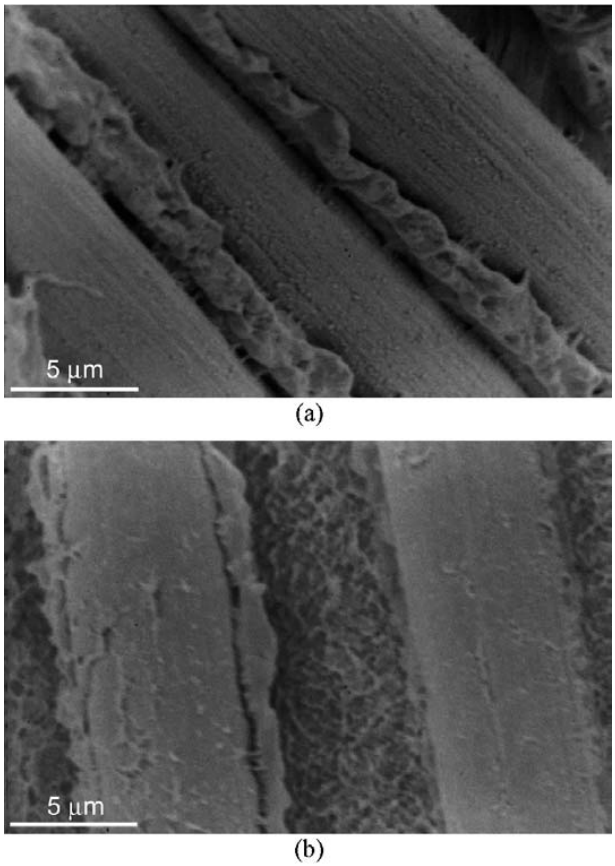

10 View of interface between polymer matrix and C fibres in composite materials with *a* GM 9255 F and *b* A 6016 matrices

development of anisotropy and locally enhances the stiffness of the matrix. This agrees with an earlier study focusing on the mechanical properties of composites of glass fibre reinforced Nylon,[20] in which the matrix was found to be stiffer in the skin region.

Fibre length distribution and fibre orientation

Figure 11 presents typical fibre length distributions for both the HDPE/C fibre composites. The HDPE GM 9255 F/C fibre composites (Fig. 11*a*) exhibit a bimodal fibre length distribution with an average fibre length of 206 μm that corresponds to a r_e of about 29, and minimum and maximum fibre lengths of 22 and 532 μm, respectively that correspond to a maximum variation interval of 510 μm. The strong reduction in fibre length is attributed to the rather long processing path suffered by the material at both the compounding and injection units. In spite of this, the values reported here may be regarded as preliminary results and further improvements in fibre length characteristics are expected following an adequate optimisation of the processing conditions. The occurrence of a bimodal distribution suggests that the final fibre length distribution is defined by two distinct degradation processes. The first is believed to be associated with the initial fibre breakage that takes place during the compounding of the composite. The second process is presumably associated with the remaining steps such as conveying from the compounding unit to the injection unit and plasticising at the injection unit, that further extends the fibre degradation phenomenon and causes the appearance of

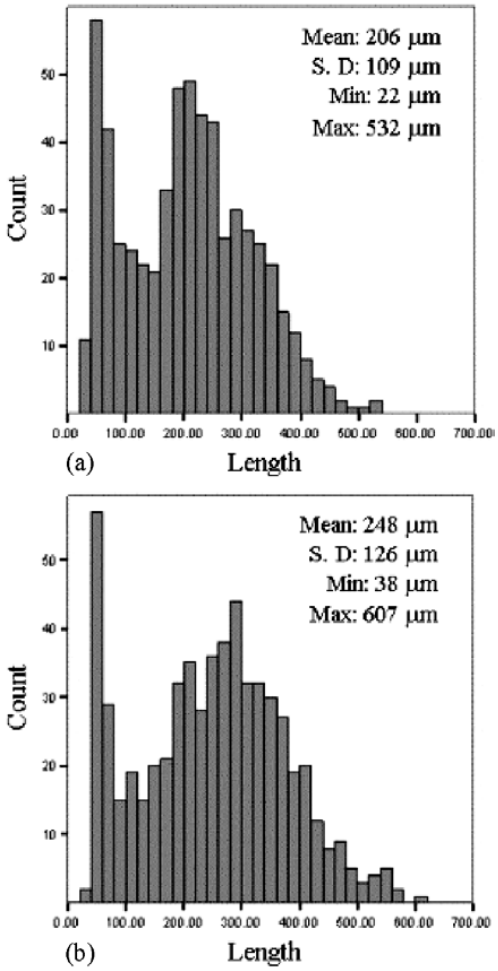

11 Fibre length distribution for HDPE/C fibre composites with *a* GM 9255 F and *b* A 6016 matrices

a large population of very short fibres at a sample mode of 45 μm.

The HDPE A 6016/C fibre composites (Fig. 11*b*) also exhibit a bimodal fibre length distribution with an average fibre length of 248 μm, which corresponds to a r_e of 35. The minimum and maximum fibre lengths are, in this case, 38 and 607 μm, respectively which corresponds to a variation interval of 569 μm. A 6016 based composites exhibit a higher fibre length and a wider fibre length distribution compared to GM 9255 F based composites. Fibre length measurements were additionally conducted for the compounds before being injection moulded. Both composites exhibit a bimodal distribution before filling of the moulding cavity. The broadness of these fibre length distributions is reduced upon injection, the reduction being more severe for the GM 9255 F based composites. In fact, before injection, these composites present an average fibre length of 250 μm and minimum and maximum fibre lengths of 25 and 688 μm, respectively. So the average fibre length is almost unchanged during filling of the mould cavity. On the other hand, before moulding, the GM 9255 F based composites exhibit an average fibre length of 238 μm and minimum and maximum lengths of 43 and 603 μm, respectively. These results indicate that the C fibres are more prone to breakage during mould filling in the GM 9255 F based composites, probably due to the higher degree of fibre/polymer interaction.

Plastics, Rubbers and Composites prc2106.3d 7/10/04 17:28:16
The Charlesworth Group, Wakefield +44(0)1924 369598 - Rev 7.51n/W (Jan 20 2003)

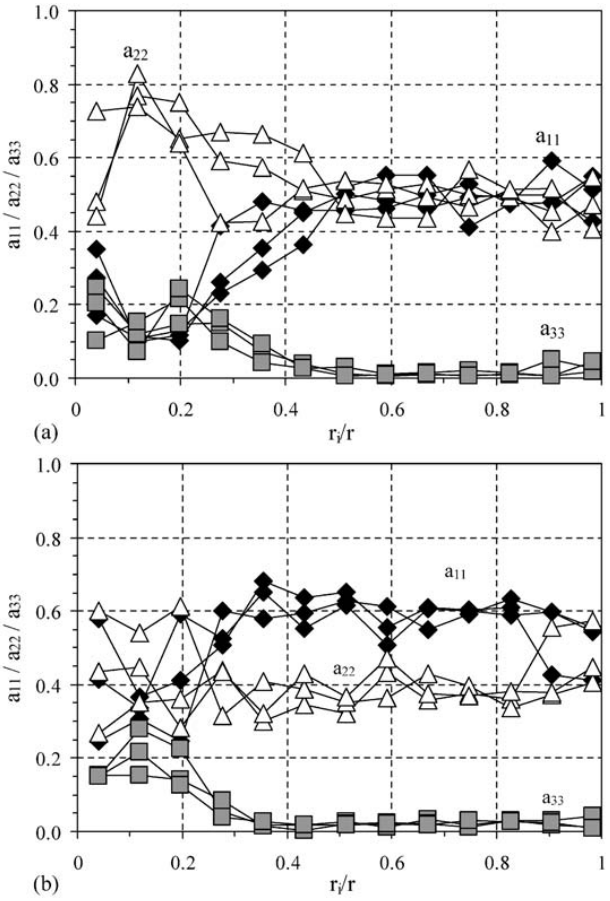

12 Fibre orientation variation along fractional half thickness (r/r_i) in terms of second-order tensor components a_{11}, a_{22} and a_{33} for HDPE/C fibre composites with *a* GM 9255 F and *b* A 6016 matrices (r/r_i=0, moulding core; r/r_i=1, mould wall)

Figure 12 presents the fibre orientation variation along half the relative cross-section thickness for both the HDPE GM 9255 F and HDPE A 6016 composites with C fibres. Note that in this figure, the fractional half thickness (r_i/r) is equal to 1 at the mould wall while at the moulding core it is equal to 0. The fibre orientation is described in terms of the second-order tensor components $\mathbf{a}_{11}$, $\mathbf{a}_{22}$ and $\mathbf{a}_{33}$, which describe the state of orientation in relation to MD, TD and ND, respectively. The HDPE GM 9255 F/C fibre composites (Fig. 12*a*) exhibit two distinct regions. The first is associated with the shell zone and is located in the $0{\cdot}5<r/r_i<1$ range. In this region, the fibre orientation in MDF is the highest, but even so considerably low. Typical values of $\mathbf{a}_{11}$ in this region are between 0·4 and 0·6. The second region exhibits poorer fibre orientation and corresponds to the moulding core, being located in the $0<r/r_i<0{\cdot}5$ range. The fibres in this region are predominantly aligned in the transverse direction to the MDF. The HDPE A 6016/C fibre composites (Fig. 12b) show a different fibre orientation profile along the moulding thickness to what is observed for the GM 9255 F based composites. In this case, the shell region is thicker, being observed in the $0{\cdot}3<r/r_i<1$ range. The fibres in this area are considerably more aligned in the MDF compared to the GM 9255 F based composites. The values of $\mathbf{a}_{11}$ are always very close to 0·6. At the core of the moulding, fibres tend to adopt an almost random state of orientation.

It is evident that both composites feature a similar shell/core morphology but with distinct fibre orientation states. This type of morphology, exhibiting a transversely orientated core, results from the occurrence of divergent flow at the mould cavity induced by the gate arrangement. After occurrence of divergent flow at the gate, significant fibre rearrangement takes place during the remaining filling of the cavity, such rearrangement being determined by the rheological behaviour of the matrix. The shear thinning character of the polymer defines its velocity gradient and consequently the fibre reorientation that takes place during flow. The higher the power law index of the polymer, the more pronounced is the velocity gradient (less flat) and the more intense will be fibre reorientation along the flow path. Computational work by Bay and Tucker[29] on various materials predicted a thicker core for the compound with less pronounced shear thinning. In the present study, the two HDPE grades differ both in their viscosity and shear thinning character. The higher viscosity HDPE GM 9255 F presents a power law index of 0·42, while the HDPE A 6016 exhibits a more pronounced shear thinning behaviour with a power law index of 0·50. Discrepancies in the core/shell dimensions between the two composites can be partially attributed to the dissimilar shear thinning characteristics. Nevertheless, the magnitude of this dissimilarity cannot be explained entirely by the differences between the two composite morphologies. Another reason that justifies this discrepancy is the higher temperature profile in the barrel (plus 35°C at the nozzle) for the higher viscosity grade. Higher melt and mould temperatures favour the development of a thicker transversely orientated core.[33] A description of the influence of processing conditions, mould design and material related variables can be found in the review by Papathanasiou.[33]

Final discussion and conclusions

This work evaluated the processability of two HDPE/C fibre composites by compounding injection moulding, the mechanical performance and its correlation with the morphology developed. The main conclusions of the present study are

1. The two composite materials produced by compounding injection moulding exhibit distinct mechanical performances. The composites with the lower viscosity HDPE grade, A 6016, exhibit higher stiffness, higher strength and superior impact performance compared to the GM 9255 F based composites. The impact behaviour of these materials is unexpectedly high when taking into account their molecular weight data compared to GM 9255 F.

2. Both composites exhibit a three layer laminated morphology that features two shell zones and a core region. The fibres in the shell zones are predominantly orientated parallel to the MDF, while in the core they are transversely orientated. Slight crystalline anisotropy of the polymer matrix in the shell zones can be observed for both cases near the mould wall. For the loading conditions employed here, the GM 9255 F matrix exhibits a poorer interfacial interaction with the C fibres compared to the A 6016 grade. The lower viscosity of the HDPE A 6016 enhances wetting of the surface of the C fibres which favours mechanical interlocking between the two phases.

Plastics, Rubbers and Composites prc2106.3d 7/10/04 17:28:20
The Charlesworth Group, Wakefield +44(0)1924 369598 - Rev 7.51n/W (Jan 20 2003)

3. Both composites display a bimodal fibre length distribution that reflects significant fibre length degradation. This bimodal character is already observed before injection into the mould cavity and is believed to occur as a result of the long conveying/plasticising path. The A 6016 based composites appear to be less prone to fibre degradation mechanisms during mould filling and present a higher average fibre length (r_e of 35 compared with 29 for the GM 9255 F grade) and a wider fibre length distribution (569 μm compared with 510 μm). In terms of fibre orientation, the GM 9255 F based composites exhibit a larger transversely orientated core (50% of the thickness compared to 30% for the A 6016 grade) and weaker orientated shell regions ($0{\cdot}4<\mathbf{a}_{11}<0{\cdot}6$ compared to $\mathbf{a}_{11}=\sim 0{\cdot}6$). The existence of a transversely orientated core results from the occurrence of divergent flow in the mould cavity induced by the gate geometry. The morphological differences observed between the two composites are explained by the dissimilar pseudo-plastic (shear thinning) behaviour of the HDPE grades and the different thermal levels of the compounds during injection moulding.

4. The different mechanical performances observed for the two materials are the result of different morphological and fibre characteristics.

5. Compounding injection moulding has been shown to be a potential processing technique to be used in rapid production of short fibre reinforced composites with enhanced fibre integrity. The values of stiffness and strength reported in the present study for the HDPE based composites are within the typical range of human cortical bone and can be regarded as interesting values for the intended orthopaedic field of application. Further improvements in mechanical performance are expected based on the use of more adequate mould designs, tailored rheological behaviour of the matrices and optimisation of the respective processing conditions.

Acknowledgements

The support of Dr Sióbhan Mathews and Dr Tony McCalla (Wolfson Centre) during CIM operation is also gratefully acknowledged. Rui A. Sousa acknowledges the financial support through grant PRAXIS XXI BD/13863/97 and the C fibres kindly supplied by Tenax Fibers GmbH.

References

1. D. Fawcett: 'A textbook of histology'; 1986, Philadelphia, PA, W.B. Saunders Co.
2. S. Weiner and H. D. Wagner: *Annu. Rev. Mater. Sci.*, 1998, **28**, 271–298.
3. R. B. Martin and D. B. Burr: 'Structure, function and adaptation of compact bone'; 1989, New York, Raven.
4. G. P. Evans, J. C. Behiri, W. Bonfield and J. D. Currey: *J. Mater. Sci. Mater. Med.*, 1990, **1**, 38–43.
5. W. Bonfield: 'Monitoring of orthopaedic implants', (ed. F. Burny and R. Pruers), 4; 1993, Amsterdam, Elsevier Science Publishers.
6. W. Bonfield: *J. Biomech.*, 1987, **20**, 1071–1074.
7. M. Wang, N. H. Ladizesky, K. E. Tanner, I. M. Ward and W. Bonfield: *J. Mater. Sci.*, 2000, **35**, 1023–1030.
8. N. H. Ladizesky, I. M. Ward and W. Bonfield: *J. Appl. Polym. Sci.*, 1997, **65**, 1865–1882.
9. R. L. Reis, A. M. Cunha, M. J. Oliveira, A. R. Campos and M. J. Bevis: *Mater. Res. Innov.*, 2001, **4**, 263–272.
10. R. A. Sousa, R. L. Reis, A. M. Cunha and M. J. Bevis: *J. Appl. Polym. Sci.*, 2002, **86**, 2866–2872.
11. G. Kalay, R. A. Sousa, R. L. Reis, A. M. Cunha and M. J. Bevis: *J. Appl. Polym. Sci.*, 1999, **73**, 2473–2483.
12. R. A. Sousa, A. L. Oliveira, R. L. Reis, A. M. Cunha and M. J. Bevis: *J. Mater. Sci. Mater. Med.*, 2003, **14**, 385–397.
13. Product information, Tenax Fibers GmbH & Co., 1999.
14. R. Clarke, N. C. Davidson and G. Archenhold: 'Flow induced alignment in composite materials', (ed. T. D. Papathanasiou and D. C. Guell), 230–292; 1997, Cambridge, Woodhead Publishing Ltd.
15. S. Advani and C. L. Tucker: *J. Rheol.*, 1987, **31**, 751–784.
16. M. J. Stevens and J. A. Covas: 'Extruder principles and operation', 2nd edn; 1995, Cambridge, Chapman & Hall.
17. J. Karger-Kocsis: 'Proceedings of the NATO Advanced Study Institute on Structure Development During Polymer Processing', (ed. A. M. Cunha and S. Fakirov); 2000, Dordrecht, Kluwer Academic Publishers.
18. B. J. Egan and O. Delatycki: *J. Mater. Sci.*, 1995, **30**, 3307.
19. J. T. Yeh and J. Runt: *J. Polym. Sci. Polym. Phys. Ed.*, 1991, **29**, 371.
20. M. W. Darlington, B. K. Gladwell and G. R. Smith: *Polymer*, 1977, **18**, 1269.
21. C. Lhymn and J. M. Schultz: *J. Mater. Sci. Lett.*, 1985, **4**, 1244.
22. J. C. Malzahn and J. M. Schultz: *Comp. Sci. Technol.*, 1986, **27**, 253.
23. D. E. Spahr, K. Friedrich, J. M. Schultz and R. S. Bailey: *J. Mater. Sci.*, 1990, **27**, 4427.
24. V. B. Gupta, R. K. Mittal, P. K. Sharma, G. Mennig and J. Wolters: *Polym. Eng. Sci.*, 1990, **10**, 16.
25. M. Akay and D. Barkley: *J. Mater. Sci.*, 1991, **26**, 2731–2742.
26. S. Toll and P.-O. Andersson: *Polym. Compos.*, 1993, **14**, 116–125.
27. Z. Yu, A. Ait-Kadi and J. Brisson: *Polymer*, 1994, **35**, 1409.
28. K.-C. Ho and M.-C. Jeng: *Plast. Rubber Compos. Proc. Applic.*, 1996, **25**, 469.
29. R. S. Bay and C. L. Tucker III: *Polym. Compos.*, 1992, **13**, 332.
30. M. Gupta and K. K. Wang: *Polym. Compos.*, 1993, **14**, 367.
31. J. Karger-Kocsis: 'Polypropylene structure, blends and composites', Vol. 3, Composites, (ed. J. Karger-Kocsis); 1995, Cambridge, Chapman & Hall.
32. B. O'Donnell and J. R. White: *Plast. Rubber Compos. Proc. Applic.*, 1994, **22**, 69.
33. T. D. Papathanasiou: 'Flow induced alignment in composite materials', (ed. T. D. Papathanasiou and D. C. Guell), 112–165; 1997, Cambridge, Woodhead Publishing Ltd.

2

Authors Queries

Journal: **Plastics, Rubbers and Composites**
Paper: **2106**
Title: **Integrated compounding and injection moulding of short fibre reinforced composites**

Dear Author
During the preparation of your manuscript for publication, the questions listed below have arisen. Please attend to these matters and return this form with your proof. Many thanks for your assistance

Query Reference	Query	Remarks
1	Author: Please supply keywords.	
2	Author: Ref. 32 is not mentioned in the text, please insert citation.	